nitrocellulose by the Southern blot method, and probed with nick-translated plasmid pPC106 (which contains the 3.2-kb Pvu II fragment of streptococcal DNA from plasmid pPC101) (Fig. 4). This probe hybridized to three Hae III fragments in the four genomic streptococcal DNA's examined (Fig. 4, lanes 1, 4, 5, and 8). The two smaller fragments (1.25 and 0.3 kb) appeared identical; however, the 1.9-kb Hae III fragment from M^+ cells was slightly, but reproducibly, larger than that from M^- streptococci (Fig. 4, lanes 4 and 5). Analysis of Pvu II digests also revealed a shortened Pvu II fragment (the 3.2-kb fragment from M^+ cells and pPC101) in DNA's from M^- cells (data not shown). This difference was estimated to be about 50 base pairs (bp). Moreover, since the 1.9-kb Hae III fragment of plasmid pPC101 was identical to that in genomic DNA from strains CS24 and CS44 (Fig. 4, lanes 4, 8, and 9), we concluded that the DNA deletion that produced pPC101 from the original pPC37 clone did not involve these particular DNA sequences.

Further analysis of Hae III–Pvu II double-digestion products revealed that a deletion of DNA was most likely responsible for the 50-bp difference observed between M^+ and M^- genomic DNA's. Since both the Hae III and Pvu II fragments were shorter in M^- DNA's, we reasoned that an inversion should change the orientation of one Hae III site relative to one of the two Pvu II sites demarking the 3.2-kb Pvu II fragment (Fig. 2). If an inversion had occurred, then Hae III–Pvu II digests of DNA from M^- and M^+ cells would differ, and Pvu II would not cleave the 1.85-kb Hae III fragment from M^- cells. Pvu II cleaved that fragment identically in both M^- and M^+ DNA (Fig. 4, lanes 2, 3, 6, and 7). Therefore, we concluded that the M^- phenotype in strains CS46 and CS64 did not arise from a DNA inversion but was probably the result of similar deletions within or adjacent to the M-protein structural gene.

Numerous traits of hemolytic streptococci exhibit phenotypic variation concomitant with changes in M protein synthesis. Capsule formation (*2*), SCFI activity (*3*), immunoglobulin G Fc receptor expression (*20*), and serum opacity activity (*2, 20*) are a few examples. Strains CS46 and CS64, in contrast to their M^+ parent strains, lack hyaluronic acid capsules and SCFI activity (*21*). The pleiotropic nature of the event that created these M^- mutants suggests that the genes responsible for these phenotypes might be under coordinate control, possibly as a virulence operon. This hypothesis is consistent with data showing that the M^- variants contain a deletion in the restriction fragment that includes the amino-terminal end of the M-protein gene. Since two independent M^- variants harbor these small deletions, which are pleiotropic and map in a common 355-bp segment of DNA (*21*), we postulate that they identify a programmed regulatory switch. Comparisons of the nucleotide sequences of the M12 gene and adjacent DNA with those from M^- variants and the M6 gene (*22*) should help clarify the mechanisms of antigenic variation exhibited by this important human pathogen.

JONATHAN G. SPANIER
S. J. C. JONES
PATRICK CLEARY
Department of Microbiology,
University of Minnesota,
Minneapolis 55455

References and Notes

1. E. W. Todd, *Br. J. Exp. Pathol.* **8**, 289 (1927).
2. P. P. Cleary, Z. Johnson, L. W. Wannamaker, *Infect. Immun.* **12**, 109 (1975).
3. D. E. Wexler, R. D. Nelson, P. P. Cleary, *ibid.* **39**, 239 (1983).
4. E. N. Fox, *Bacteriol. Rev.* **38**, 57 (1974).
5. R. C. Lancefield, *J. Immunol.* **89**, 307 (1962).
6. J. Jacks-Weis, Y. Kim, P. P. Cleary, *ibid.* **128**, 1897 (1982).
7. E. W. Todd and R. C. Lancefield, *J. Exp. Med.* **48**, 751 (1928).
8. S. Rothbard and R. F. Watson, *ibid.* **87**, 521 (1948); P. J. Wormald, *J. Hyg.* **54**, 89 (1956).
9. W. R. Maxted and H. A. Valkenburg, *J. Med. Microbiol.* **2**, 199 (1969); W. R. Maxted, in *Streptococci*, F. A. Skinner and L. B. Quesnel, Eds. (Academic Press, London, 1978), pp. 107–125; P. P. Cleary, D. Johnson, L. W. Wannamaker, *J. Infect. Dis.* **140**, 747 (1979).
10. T. Maniatis *et al.*, *Cell* **15**, 687 (1978).
11. M. Feiss, D. A. Siegele, C. F. Rudolph, S. Frackman, *Gene* **17**, 123 (1982).
12. B. Hohn, in *Methods in Enzymology*, R. Wu, Ed. (Academic Press, New York, 1979), vol. 68, pp. 299–309.
13. T. Maniatis, E. F. Fritsch, J. Sambrook, *Molecular Cloning: A Laboratory Manual* (Cold Spring Harbor Laboratory, Cold Spring Harbor, N.Y., 1982), p. 504.
14. D. J. Kemp and A. F. Cowman, *Proc. Natl. Acad. Sci. U.S.A.* **78**, 4520 (1981).
15. J. G. Spanier and P. P. Cleary, *J. Exp. Med.* **152**, 1393 (1980).
16. J. Messing, *Recombinant DNA Tech. Bull.* **2**, 43 (1979).
17. J. Vieira and J. Messing, *Gene* **19**, 259 (1982).
18. V. A. Fischetti, E. C. Gotschlich, G. Siviglia, J. B. Zabriskie, *J. Exp. Med.* **144**, 32 (1976).
19. R. C. Lancefield, *ibid.* **106**, 525 (1957).
20. L. A. Burova, L. E. Ravdonikas, P. Christensen, C. Schalen, A. A. Totolian, *Acta Path. Microbiol. Immunol. Scand. Sect. B* **91**, 61 (1983).
21. J. G. Spanier, S. J. C. Jones, P. Cleary, unpublished data.
22. J. R. Scott and V. A. Fischetti, *Science* **221**, 758 (1983).
23. M. D. Moody, J. Padula, D. Lizana, C. T. Hall, *Health Lab. Sci.* **2**, 149 (1965).
24. R. C. Lancefield, *J. Exp. Med.* **47**, 91 (1928).
25. J. G. Spanier and P. P. Cleary, *Virology* **130**, 514 (1983).
26. Supported by Public Health Service grant AI16722 from the National Institute of Allergy and Infectious Diseases. J.G.S. was supported by Public Health Service Training grant 5T32HLI07114 as a postdoctoral trainee from the National Heart and Lung Institute.

23 January 1984; accepted 6 June 1984

Scintigraphy of Normal Mouse Ovaries with Monoclonal Antibodies to ZP-2, the Major Zona Pellucida Protein

Abstract. *The zona pellucida is an extracellular glycocalyx, made of three sulfated glycoproteins, that surrounds mammalian oocytes. Parenterally administered monoclonal antibodies specific for ZP-2, the most abundant zona protein, localize in the zona pellucida. When labeled with iodine-125, these monoclonal antibodies demonstrate a remarkably high target-to-nontarget tissue ratio and provide clear external radioimaging of ovarian tissue.*

The advent of monoclonal antibodies has markedly improved the ability of external radioimaging techniques to locate tumors (*1, 2*) and to identify certain noncancerous diseases (*3*). However, the success of these studies is highly dependent on the concentration and distribution of the antigen recognized by the antibody. Many monoclonal antibodies detect antigens only when the latter are present in at least 10^4 or 10^5 copies per cell, and most cancer-associated antigens are present in targeted as well as nontargeted tissue. This lack of specificity has hampered the usefulness of such antibodies for immunoscintigraphy. Much better radioimaging might be expected for tumor-specific antigens, as has been reported with anti-idiotypic antibodies in B-cell leukemias (*4*), or for normal tissue antigens that are found exclusively in a particular organ (*5, 6*).

During growth and development, mammalian oocytes synthesize and secrete an extracellular zona pellucida (ZP). Each murine ZP is composed of three sulfated glycoproteins known as ZP-1, ZP-2, and ZP-3, which have molecular weights of 185,000, 140,000 and 83,000, respectively (*7, 8*). The ZP has three apparent functions: (i) mediation of species-specific sperm binding at the time of fertilization, (ii) blockage of postfertilization polyspermy, and (iii) protection of the preimplantation embryo as it passes down the oviduct (*9*). ZP-3 composes 19 percent of the ZP mass and may be the species-specific sperm receptor (*10*). ZP-2, which makes up almost 50 percent of the ZP, is biochemically modi-

fied in conjunction with the postfertilization block to polyspermy (*11*). As yet, ZP-1 has no known function.

We recently developed a battery of rat monoclonal antibodies specific for murine ZP-2 (*6*) and ZP-3 (*12*). These immunological reagents have been used to demonstrate that the ZP proteins are immunologically distinct from other extracellular matrix proteins. In addition, it appears from indirect immunofluorescence studies that the ZP proteins are found only in ovarian tissue and, within the ovary, only in the ZP surrounding growing oocytes (*6*). These results suggest that an appropriately labeled monoclonal antibody to ZP might, after parenteral administration, localize in ovarian tissues. Furthermore, the high concentration of the ZP proteins may provide high target-to-nontarget tissue ratios for immunoscintigraphy. The use of rat monoclonal antibodies to a mouse antigen is analogous to the use of heterologous antibodies in clinical diagnostic immunoscintigraphy.

Several rat monoclonal antibodies to mouse ZP have been isolated and chromatographically purified. One cell line, IE-3, secretes an immunoglobulin G_{2a} (IgG_{2a}) antibody that specifically immunoprecipitates ZP-2 (Fig. 1A). Binding studies with ovulated eggs demonstrate that antibody to ZP-2 has a dissociation constant of $2 \times 10^{-10} M$ and binds to 1.3×10^8 sites, or approximately 2 percent of the ZP-2 molecules per ZP (*6*). Six-week-old female NIH Swiss mice were parenterally injected with 250 μg of this monoclonal antibody and killed after 6 days. In frozen ovarian sections stained with rhodamine-conjugated antibody to rat IgG we observed that the monoclonal antibody to ZP-2 had localized in the ZP surrounding oocytes (Fig. 1C).

The vasculature of the normal ovary may have greatly facilitated localization of the antibodies to ZP-2 in the ZP in situ. The ovaries receive approximately 0.2 percent of the cardiac output—an amount exceeded on a weight basis only by the kidneys (*13*). The ovarian capillary system penetrates the thecal layers of the growing follicles, but goes no farther than the basement membrane that encloses the granulosa cells surrounding the maturing oocytes. Nutrients and larger macromolecules must pass from the capillaries to the oocyte by passive diffusion through the semipermeable ZP. This process is facilitated, particularly for macromolecules, by the high permeability of ovarian capillaries (*13*). Thus the vascularization of the normal ovary may resemble that of tumors, and this may, in part, account for the successful localization of antibodies to ZP-2 in the ovarian ZP.

To investigate this phenomenon, we labeled purified monoclonal antibody with radioiodinated Bolton and Hunter reagent (*6*) and injected approximately 2.7 μCi into each of 15 female and two male NIH Swiss mice. Groups of three females were killed at different intervals and the amount of radioactivity in various tissues was determined (Fig. 2A). Initially there was a great deal of radioactivity in the liver, gastrointestinal

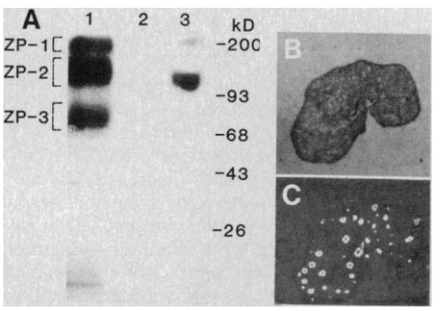

Fig. 1. (A to C) Monoclonal antibodies specific for ZP-2. (A) Mouse ZP-2 monoclonal antibodies from rat cell line IE-3 were chromatographically purified (*6*) and used to immunoprecipitate ^{125}I-labeled ZP's. Reaction mixtures contained 50 μg of IE-3 antibody and 2.7×10^6 count/min of ^{125}I-labeled ZP's in a final volume of 100 μl of phosphate-buffered saline containing 1 percent Triton X-100, bovine serum albumin (1 mg/ml), and 1 m*M* phenylmethylsulfonyl fluoride (*6*). The mixtures were incubated for 2 hours at 20°C; then 20 μl of sheep antibody to rat IgG was added and the incubation was continued for 16 hours at 4°C. Samples were washed, solubilized, and analyzed by 10 percent sodium dodecyl sulfate–polyacrylamide gel electrophoresis. After being fixed in 10 percent trichloroacetic acid, 10 percent acetic acid, and 30 percent methanol for 1 hour, the gels were dried and exposed to x-ray film (*6*). Lane 1 shows the ^{125}I-labeled ZP's before immunoprecipitation; lane 2, immunoprecipitation with 50 μl of control ascites fluid; and lane 3, immunoprecipitation with the ZP-2–specific monoclonal antibody from the IE-3 cell line. (B) NIH Swiss female mice were injected intraperitoneally with 250 μg of monoclonal antibody to ZP-2 in phosphate-buffered saline. Six days later the mice were killed and frozen sections of their ovaries were obtained and stained with methylene blue. Oocytes in various stages of maturation are visible along with their surrounding ZP's. (C) An affinity-purified, rhodamine-conjugated (Jackson Immunoresearch) rabbit antibody to mouse IgG was used with a Zeiss Photomicroscope III equipped for epifluorescence (*6*) to detect monoclonal antibodies to ZP-2. Animals injected with control ascites fluid did not show fluorescent staining of their ovaries.

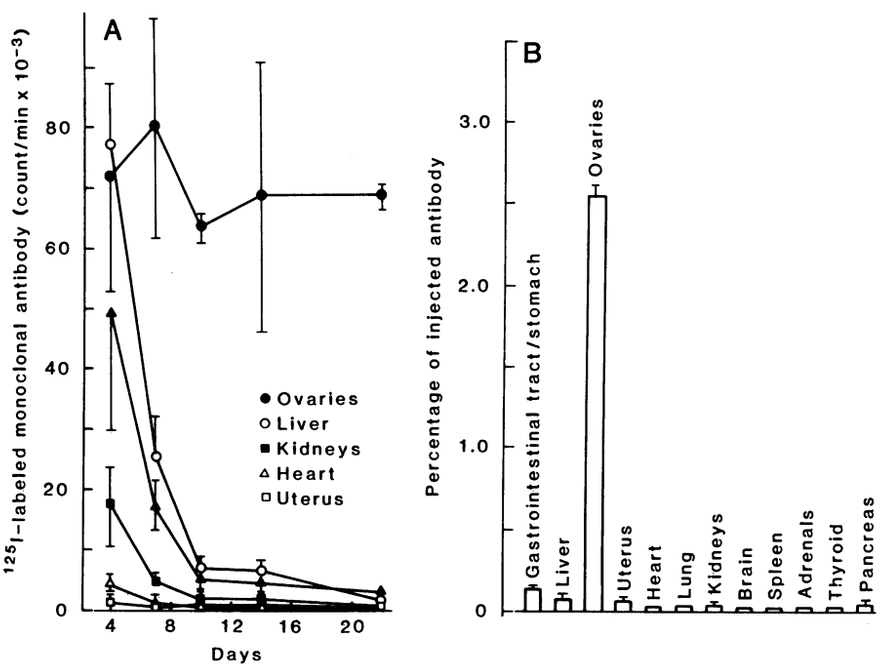

Fig. 2. Localization of ^{125}I-labeled rat monoclonal antibody to mouse ZP-2 in the ovary. (A) Chromatographically purified monoclonal antibodies to ZP-2 were labeled with ^{125}I-labeled Bolton and Hunter reagent, desalted on a PD-10 (Pharmacia) column equilibrated with 0.1 percent gelatin in phosphate-buffered saline, and dialyzed against H_2O and used immediately (*6*). Fifteen 3-week-old female Swiss mice were each injected with 2.7 μCi (6.0×10^8 cpm/μg) of ^{125}I-labeled monoclonal antibody. Sets of three mice chosen arbitrarily were killed on days 4, 7, 10, 14, and 22. Tissues were dissected out and counted in a Multi-Prias Auto Gamma System (Packard) with 70 percent efficiency. The mean number of counts for the three animals is presented at each time point; standard errors are shown where large enough to indicate. (B) A more extensive dissection was carried out on the animals killed day 22. Total body retention was 3.0 percent of the injected dose.

tract, and heart, but by day 10 radioactivity had declined to less than 0.2 percent of the administered dose. However, the amount of radioactivity in the ovaries remained high during the entire 22-day period, ranging from 3.9 to 11.4 $\times 10^4$ count/min. The variability may have been due to variations in the pharmacokinetics of antibody metabolism or to different numbers of mature oocytes in outbred strains of mice. However, after day 4 the relative distribution in tissues was fairly constant among animals, with most of the radioactivity in the ovaries, followed by the liver, gastrointestinal tract, heart, and kidneys (Fig. 2A).

The difference in radioactivity between the ovaries and other tissues was maximal 22 days after injection (Fig. 2B). Even after this extended period 2.6 percent of the initial 2.7 μCi was still associated with the ovaries (compared to 0.12 percent in the liver). When comparisons are made on the basis of tissue mass the radioactivity ratio between the two 2-mg ovaries and the 950-mg liver is particularly striking. The ovaries contained 1300 percent of the injected dose per gram of tissue, compared to 0.11 percent for the liver. This mass ratio between target and nontarget tissue is considerably greater than ratios reported for the radioimaging of tumor or normal tissue antigens with monoclonal antibodies (*1*, *2*).

In addition to the vascular permeability of the ovary, the following other factors may account for our findings: (i) a high affinity of the monoclonal antibody for the ZP; (ii) the fact that ZP-2 is found only in the ovary; (iii) the low rate of catabolism (*14*) of the intraovarian antibodies to ZP, which permitted us to determine their biodistribution as long as 3 weeks after the initial injection; and (iv) the high concentration of ZP-2 in the ZP. In mature oocytes ZP's contain 5 ng of protein, of which 47 percent is ZP-2 in a volume of roughly 2×10^{-13} liter. Thus each ZP has approximately 6×10^9 molecules of ZP-2 at a concentration of greater than 85 m*M*; in vitro studies suggest that at least 2 percent of these molecules are available for antibody binding (*6*). However, the 5000 to 6000 oocytes in each ovary (*15*) are at different stages of development and have ZP's of various thicknesses; therefore the amount of ZP-2 per ovary is difficult to estimate.

The two male mice were also killed on day 22. Although they weighed 27 percent more than their female counterparts, they had 37 percent less radioactivity in the composite of their major organs. This difference could be accounted for in large part by the lack of localization of radioactivity in a particular tissue. The testes contained only 0.03 percent of the injected radioactivity. However, the males had several times more background radioactivity in their other major organs than their female counterparts. Thus the ovary appears to trap the ^{125}I-labeled monoclonal antibody and may lessen uptake by other organs.

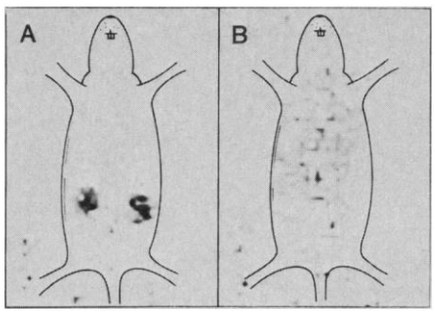

Fig. 3. Ventral gamma camera images of NIH Swiss mice obtained 22 days after intraperitoneal injection of approximately 2.7 μCi of ^{125}I-labeled monoclonal antibody to ZP-2. (A) Female animal with both ovaries clearly visible. (B) Male animal with only nonspecific body background activity present. Each image was collected for 30 minutes, integrated into a 64 by 64 pixel matrix, and interpolated to a 256 by 256 matrix without computer smoothing. Spontaneous background was subtracted to eliminate camera artifacts due to prolonged imaging times, and both images were scaled to a common maximum pixel value. These animals were subsequently dissected and the distribution of radioactivity among tissues was determined (Fig. 2).

We performed immunoscintigraphy on female and male mice on day 22 immediately after they were killed by using a gamma camera equipped with a 0.25-inch pinhole collimator positioned a standard distance above the ventral surface of each animal. A 20 percent energy window was centered over the low-energy gamma and x-rays of ^{125}I, and the data (30 minutes per image) were collected with a digital computer into a 64 by 64 pixel matrix. Because of the excellent target-to-nontarget tissue ratio, body background subtraction techniques were not necessary and no contrast enhancement was used.

The ovaries were clearly visualized in the female mouse, with other tissue exhibiting only minimal background activity (Fig. 3). There was no localization of radioactivity in the male mice, as determined by scintigraphy or tissue counting. Target-to-nontarget tissue ratios in the female mice were determined by computer analysis of the scintiphotos to be 4.9 and 4.4 to 1.0 for the left and right ovaries, respectively (an identical area between the ovaries was used as a representative background region). The reasons for the target-to-nontarget ratio being lower than the ratio obtained from tissue counting may be the small size of the ovaries, their dorsal location (resulting in attenuation of the low-energy gamma rays by intervening tissue), and the fact that scattered photons may contribute to the observed body background radiation. In addition, a rectangular area encompassing the ovaries, which necessarily included a minimal background area, was used for the computer analysis. This decreased the calculated target radioactivity per unit of area and may have further contributed to an underestimation of the true target-to-nontarget ratio.

With the exception of monoclonal antibodies specific for certain granulocytic surface antigens (*4*, *5*), other monoclonal antibodies react with nontarget tissues, albeit to a lesser extent (*1–3*, *16*). In contrast, the antibodies to ZP react only with female germ line cells, and thus not only have organ specificity but also cell and sex specificity. These antibodies, or their Fab fragments, should be excellent vehicles for site-specific delivery of cancer therapeutic agents or for localized ablative radiotherapy. Germ cell malignancies occur primarily in young women and constitute 5 percent of all ovarian tumors (*17*). Although it is not known whether these tumors synthesize ZP protein, the surrounding oocytes appear to have normal ZP's and thus would serve as a target for the monoclonal antibodies. The LT/Sv strain of mice, which has a 50 percent incidence of spontaneous intraovarian teratomas (*18*), may be useful for testing immunological delivery of drugs to germ line tumors. These monoclonal antibodies may also provide a noninvasive diagnostic tool: their failure to localize would suggest abnormal ovarian function. Furthermore, specific binding of the antibodies to the ZP has been shown to provide an effective, long-term, reversible block to fertilization (*19*).

IAIN J. EAST
Laboratory of Chemical Biology, National Institute of Arthritis, Diabetes, Digestive and Kidney Diseases, Bethesda, Maryland 20205
ANDREW M. KEENAN
STEVEN M. LARSON
Department of Nuclear Medicine, Clinical Center, National Institutes of Health, Bethesda, Maryland 20205
JURRIEN DEAN
Laboratory of Cellular and Developmental Biology, National Institute of Arthritis, Diabetes, Digestive and Kidney Diseases

References and Notes

1. R. W. Baldwin and M. V. Pimm, *Cancer Metas. Rev.* **2**, 89 (1983); A. A. Epenetos *et al.*, *Br. J. Cancer* **46**, 1 (1982); T. Ghose, S. T. Norvell, J. Aquine, *Cancer Res.* **40**, 3018 (1980); S. M. Larson *et al.*, *J. Nucl. Med.* **24**, 123 (1983); G. N. Sfakianakis and F. H. DeLand, *ibid.* **23**, 840 (1980).
2. D. M. Goldenberg, E. E. Kim, F. H. DeLand, J. R. van Nagell, Jr., N. Javadpour, *Science* **208**, 1284 (1980); E. E. Kim *et al.*, *Cancer Res.* **40**, 3008 (1980); S. E. Order *et al.*, *Cancer (Philadelphia)* **35**, 1487 (1975).
3. B. A. Khaw, J. T. Fallon, H. W. Strauss, E. Haber, *Science* **209**, 295 (1980); E. Haber, *Pharmacology* **32**, 1967 (1980).
4. R. A. Miller, D. G. Maloney, R. Warnke, R. Levy, *N. Engl. J. Med.* **306**, 517 (1982); R. A. Warnke *et al.*, *ibid.* **309**, 1275 (1983).
5. L. L. Houston, R. C. Newinski, I. D. Berstein, *J. Immunol.* **125**, 837 (1980).
6. I. J. East and J. Dean, *J. Cell Biol.* **98**, 795 (1984).
7. J. D. Bleil and P. M. Wassarman, *Dev. Biol.* **76**, 185 (1980).
8. S. Shimizu, M. Tsuji, J. Dean, *J. Biol. Chem.* **258**, 5858 (1983).
9. R. Yanagimachi, in *Fertilization and Embryonic Development in Vitro*, L. Mostroianni, Jr., and J. D. Biggers, Eds. (Plenum, New York, 1981), pp. 81–182.
10. J. D. Bleil and P. M. Wassarman, *Cell* **20**, 873 (1980).
11. ———, *Dev. Biol.* **86**, 189 (1981).
12. I. J. East and J. Dean, *J. Cell Biol.* **97**, 183a (1983); I. J. East, B. Gulyas, J. Dean, unpublished observations.
13. W. E. Ellinwood, T. M. Nett, G. D. Niswender, in *The Vertebrate Ovary*, R. E. Jones, Ed. (Plenum, New York, 1978), pp. 583–614.
14. G. Froese, I. Berczi, L. G. Israels, *Immunology* **45**, 303 and 313 (1982); D. A. Scheinberg and M. Strand, *Cancer Res.* **43**, 265 (1983).
15. M. J. Faddy, E. C. Jones, R. G. Edwards, *J. Exp. Zool.* **197**, 173 (1976).
16. R. Levy and R. A. Miller, *Fed. Proc. Fed. Am. Soc. Exp. Biol.* **42**, 2650 (1983); G. Poste and R. Kirsh, *Biotechnology* **1**, 869 (1983).
17. R. C. Young, R. C. Knapp, C. A. Perez, in *Cancer: Principles and Practice of Oncology*, V. T. DeVita, Jr., S. Hellman, S. A. Rosenberg, Eds. (Lippincott, New York, 1982), pp. 884–913.
18. L. C. Stevens and D. S. Varnum, *Dev. Biol.* **21**, 364 (1970); ———, E. M. Eicher, *Nature (London)* **269**, 515 (1977).
19. I. J. East, D. R. Mattisen, J. Dean, *Dev. Biol.* **104**, 49 (1984).

20. We thank R. Simpson and D. Mattison for critical reading of the manuscript and B. Richards for expert preparation of the manuscript.

1 March 1984; accepted 1 June 1984

Identification of DNA Sequence Responsible for 5-Bromodeoxyuridine-Induced Gene Amplification

Abstract. *Bromodeoxyuridine (BrdUrd) treatment of the prolactin nonproducing subclone of GH cells (rat pituitary tumor cells) induces amplification of a 20-kilobase DNA fragment including all of the prolactin gene coding sequences. This amplified DNA segment, which is flanked by two unamplified regions, thus designates a unit of BrdUrd-induced amplified sequence. Cloned DNA segments, 10.3 kilobases long, from the 5′ end of the rat prolactin gene of BrdUrd-responsive and -nonresponsive cells, were ligated to the thymidine kinase gene of herpes simplex virus type 1 (HSV1TK), and the hybrid DNA was transferred to thymidine kinase–deficient mouse fibroblast cells by transfection. The HSV1TK gene and the rat prolactin gene were amplified together in drug-treated transfectants carrying the hybrid DNA HSV1TK gene and rat prolactin gene of BrdUrd-responsive GH cells. These results suggest that the 10.3-kilobase DNA segment at the 5′ end of the rat prolactin gene of BrdUrd-responsive GH cells carries the information for drug-induced gene amplification (amplicon) and that another gene, such as the HSV1TK gene, is also amplified when the latter is placed adjacent to this segment.*

Amplification of specific gene sequences during normal developmental processes or in response to cytotoxic agents are observed in several eukaryotic cell systems (*1–4*). The exact mechanism of such amplification of specific genes is not yet clear. A 20-kilobase (kb) length of DNA including all of the coding sequences and about 3.5 kb of the 5′ end and about 7 kb of the flanking regions of the 3′ end of the rat prolactin (rPRL) gene are amplified in bromodeoxyuridine (BrdUrd)-treated PRL-nonproducing (PRL^-) GH cells (rat pituitary tumor cells) (Fig. 1) (*5–8*). The reversible (*8*) nature of the amplification process suggests that BrdUrd treatment of cells generates a signal either within or in the immediate neighborhood of the 20-kb amplified sequences that leads to such preferential DNA replication in this region of the chromosome. To substantiate this concept, we ligated cloned DNA segments from the neighborhood of the rPRL gene of BrdUrd-responsive and -nonresponsive cells to the thymidine kinase (TK) gene of herpes simplex virus type 1 (HSV1TK) and transferred the hybrid DNA to thymidine kinase–deficient $LMTK^-$ mouse fibroblast cells by transfection (*9*).

The construction of hybrid DNA containing the rPRL and HSV1TK gene sequences is outlined in Fig. 1. Table 1 shows the characteristics of the hybrid DNA, which carries a constant region consisting of the HSV1TK gene and a variable region consisting of the 10.3-kb DNA fragment from the 5′ end of the rPRL gene of GH cell strains that are responsive and nonresponsive to BrdUrd (Fig. 1).

The HSV1TK gene does not show significant sequence homology to the mouse fibroblast TK gene (Figs. 2 and 3). However, DNA isolated from TK^+ transfectants derived with hybrid DNA generate positive signals in dot-hybridization analysis when probed with ^{32}P-labeled HSV1TK DNA (Fig. 2) (*10*). These results suggest that the HSV1TK gene is indeed transferred to mouse fibroblast cells. The hypoxanthine-aminopterin-thymidine (HAT)-resistant phenotype of the transfectants further substantiates that the HSV1TK gene is also

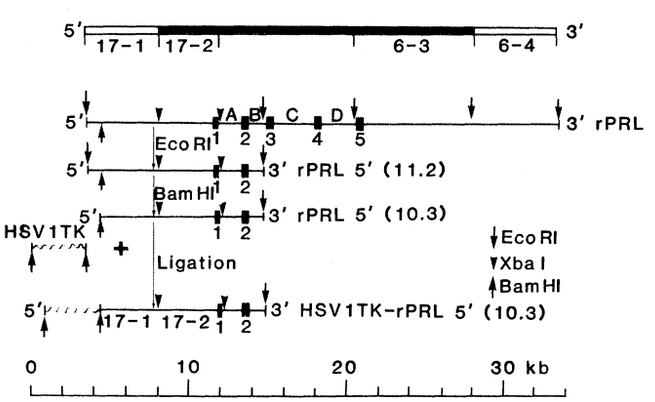

Fig. 1. Construction of hybrid DNA with the HSV1TK gene and the rPRL gene 5′ end fragment of PRL^+ and PRL^- GH cells. High molecular weight DNA (40 μg) (*12*) from PRL^+ (GH_3) and PRL^- ($F_1BGH_12C_1$) cells were digested with Eco RI, and fragments were separated on a 1 percent low-melting agarose gel. The 11-kb fragments of the genomic DNA were extracted from the gel and cloned in the Eco RI site of λ Charon 4A (*13*). Recombinant phage plaques were screened for the $[^{32}P]cDNA_{PRL}$-hybridizable sequences (*14*). The 11-kb DNA insert from the recombinant clones of PRL^+ and PRL^- GH cells were then digested with Bam HI and ligated to HSV1TK DNA to generate the hybrid DNA fragments for subsequent transfection. The HSV1TK DNA was released from the recombinant plasmid pBR322–HSV1TK (*15*) DNA by digestion with Bam HI followed by separation on 1 percent agarose gel and extraction (*7*). The top sketch shows the amplified (closed area) and unamplified (open area) regions of the PRL gene and its neighboring sequences in BrdUrd-treated GH cells. The second sketch from the top shows the organization of the rPRL gene. Closed blocks numbered 1 to 5 are exons, and letters A to D designate the four introns in the rPRL gene.